Analysis of Predictions for the Catalytic Mechanism of Ribosomal Peptidyl Transfer†

Stefan Trobro and Johan Åqvist*

Department of Cell and Molecular Biology, Uppsala University, Biomedical Center, Box 596, SE-751 24 Uppsala, Sweden

Received March 17, 2006; Revised Manuscript Received April 21, 2006

ABSTRACT: The reaction mechanism of peptide bond formation on the ribosome is now becoming established by results from both experiments and computer simulations. Here, we analyze predictions from molecular dynamics simulations, as well as from new crystal structures, and examine their implications for the mechanisms of peptidyl transfer and peptidyl-tRNA hydrolysis. A number of computational predictions for the peptidyl transfer reaction, including quantitative energetics, stereochemistry, hydrogen bonding network, and role of solvent molecules, are found to be supported and confirmed by kinetic and structural data. The results show that this type of reaction calculations can provide important links between structure and function that cannot be obtained by experimental means.

The large ribosomal subunit catalyzes peptide bond formation in the protein synthesis process. The determination of high-resolution X-ray structures (*1*, *2*) of the large subunit in bacterial ribosomes have finally made it possible to examine whether the wealth of accumulated biochemical data for the peptidyl transfer reaction can be rationalized on the atomic scale. The large subunit cocrystallized with modified aminoacylated tRNA fragments as substrate and product analogues (*3*−*6*) or, more recently, with modified tRNA phosphodiesters as transition state analogues (*6*, *7*) have all revealed a clearly defined active site for peptidyl transfer between A- and P-site substrates during elongation. The universal 3′-CCA end of tRNA base-pairs with residues in domain V of the 23S rRNA and brings the amino acid ribose esters down to the beginning of the peptide exit tunnel ∼20 Å below the interface to the small subunit. No ribosomal protein comes within ∼18 Å of the active site, and no conserved metal ion contacting the substrates is observed in the crystallographic structures. The overall impression is that of a rather chemically inert active site devoid of ions or bases that can activate the proton transfers needed both for peptidyl transfer and for hydrolysis of aminoacylated tRNA in peptide relase.

The recent development of a stopped flow assay (*8*) with full ribosomes and puromycin as the A-site substrate enabled measurement of the rate of peptidyl transfer alone and established that the ribosome catalyzes peptide bond formation by a factor of $\sim 10^6$, or by about 8 kcal/mol. Arrhenius plots also showed that, while the activation enthalpy is increased in the ribosome, a large reduction of the activation entropy appears to be responsible for the overall catalysis (*9*). While it is clear that peptide bond formation begins with the attack of the neutral A-site amine nitrogen on the P-site ribose ester carboxyl carbon, little has been known about the detailed nature of the reaction pathway. Is the attacking nitrogen deprotonated as the new N−C bond is formed, and what is then acting as a base in the reaction? Is the transient tetrahedral intermediate formed in the *R* or *S* configuration? What does the (chemically) rate-limiting transition state look like, and foremost, how does the ribosome stabilize it in terms of structure and energetics? These questions have recently been addressed by computer simulations (*10*), mutation assays (*8*, *11*, *12*), and kinetic isotope measurements (*13*), as well as new crystallographic experiments (*6*, *7*).

It has long been known that, although 2′-deoxyadenine tRNAs can bind to the P-site, they are unable to promote peptidyl transfer to the A-site substrate (*14*). Replacment of the P-site O2′ with F, thus retaining an H-bond acceptor but losing the donor capability, was also recently found to impair peptidyl transfer and led Weinger et al. to suggest that the O2′ may be involved in proton transfer to the leaving group (*12*). Independently, we found by computer simulations that the P-site O2′ group could indeed act as a proton shuttle, and that this mechanism was catalyzed by about 7 kcal/mol compared to the same reaction in water (*10*). Similar conclusions were also reached in ref *25*. Furthermore, our calculations showed that only the *S*-enantiomer of the transient intermediate would allow facile proton shuttling to the leaving group. These molecular dynamics (MD)[1] simulations utilized an initial superposition of two structures (1FG0 and 1M90) (*3*, *5*), each containing one substrate, and also showed a significant reduction of the activation free entropy in the ribosome compared to water, as found experimentally (*9*).

The MD simulations thus showed a complete agreement with kinetic measurements and for the first time allowed the energetics of ribosomal catalysis of peptidyl transfer to be

† Support from the Swedish Research Council (VR) and the Swedish Foundation for Strategic Research (SSF/Rapid) is gratefully acknowledged.

* To whom correspondence should be addressed. Phone, +46 18 471 4109; fax, +46 18 536971; e-mail, aqvist@xray.bmc.uu.se.

[1] Abbreviations: MD, molecular dynamics; EVB, empirical valence bond; FEP, free energy perturbation; TI, tetrahedral intermediate; TS, transition state; RF, release factor.

10.1021/bi0605383 CCC: $33.50
Published on Web 05/20/2006

quantitatively examined on the atomic scale. Subsequently, crystal structures of complexes with new transition state analogues, also showing *S*-symmetry, as well as reactant state analogues, have been reported and their mechanistic interpretations discussed (*6*, *7*). In view of these new data, it is highly interesting to analyze the emerging predictions regarding the mechanism of peptidyl transfer and also of aminoacyl-tRNA hydrolysis. Here, we examine the results of both earlier and new computer simulations, as well as data from recent crystal structures and other experiments, and discuss their implications for the two reactions catalyzed by the peptidyl transferase center. We find very convincing agreement between theoretical and experimental predictions for the peptidyl transfer mechanism, and it is clear that computational analysis of reaction energetics can provide links between structure and function that are otherwise difficult to obtain by experimental means.

MATERIALS AND METHODS

Molecular dynamics calculations were carried out at 300 K with the program Q (*15*) using essentially the same protocols as described previously, employing the CHARMM22 force field (*16*) with additional partial charges from ab initio 6-31G(d) calculations (*10*). The system was prepared by selecting all residues in the 1VQP structure (*7*) with atoms within a 24 Å radius from the phosphorus atom in the TS analogue (RAP). The RAP molecule was converted to the *S*-tetrahedral intermediate with CCA-Phe in the A-site and CCA-Gly in the P-site. All Sr^{2+} ions were converted to Mg^{2+} ions, and all phosphate linkages, ions, and parts of ribosomal proteins outside 18 Å were neutralized as described earlier. The system was solvated by adding ~400 water molecules and finally contained ~7000 atoms. Outside the 24 Å system boundary, atoms were restrained to their initial positions with a 100 kcal/(mol Å^2) harmonic force constant, and nonbonded interactions across the system boundary were not calculated. Water molecules close to the sphere boundary were restrained to reproduce the correct density and polarization (*15*, *17*). No interaction cutoffs were applied to reacting fragments, while for other interactions, a multipole expansion treatment (*18*) of long-range electrostatics (beyond 10 Å) was employed.

The reaction free energy surface was described by the EVB method (*19*, *20*) with calibration of the uncatalyzed water reaction energetics as described earlier (*10*). Both the ribosome and water systems were heated from 0−300 K in a stepwise fashion with initial random velocities from a Maxvell−Boltzmann distribution. The systems were then equilibrated in the tetrahedral intermediate state for 500 ps at 300 K with a 1 fs time step. The reaction free energy profiles in water and in the solvated ribosome model were calculated with the free energy perturbation/umbrella sampling method (*20*). Each free energy perturbation calculation for the entire reaction comprised 102 discrete steps with a 20 ps trajectory generated at each step, and the trajectories were initiated at the tetrahedral intermediate and propagated toward reactants and products.

RESULTS AND DISCUSSION

Catalytic Mechanism and Energetics. Initially, it was proposed that the N3 atom of the universally conserved ribosomal base A2451 (*Escherichia coli* numbering) would function as a general base during catalysis, by abstracting a proton from the attacking α-amino group of the A-site substrate (*13*, *21*). However, this prediction appeared wrong in light of new structural (*6*, *7*) and mutational (*22*) data, as well as our recent computational analysis (*10*). The latter showed that the distance between A2451 N3 and the attacking amino group was somewhat too large and that the proton transfer to the adenine was also disfavored due to a lack of stabilization of the protonated adenine. The cost of proton transfer from the N-protonated intermediate to A2451 N3 is calculated to be 7.5 ± 0.5 kcal/mol higher in the ribosome than for proton transfer to the base in water, showing that the pK_a of A2451 is not raised as would be required for such a mechanism (Figure 1). That the two groups lie just outside hydrogen bonding distance from each other is also confirmed by recent structures of complexes with TS analogues (*6*, *7*).

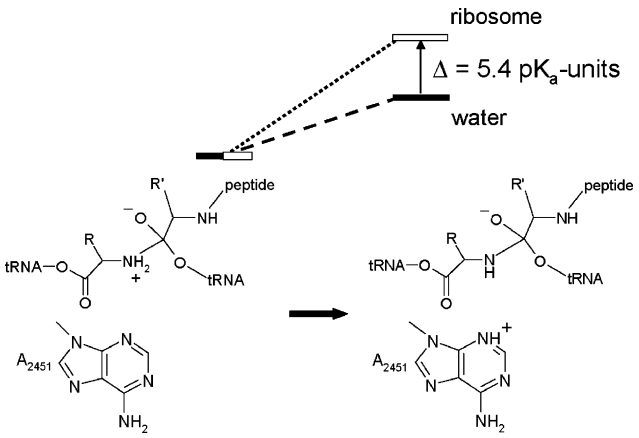

FIGURE 1: Energetics of the A2451 general base mechanism. Free energy perturbation calculation of the cost of proton transfer from the zwitterionic (dipolar) tetrahedral intermediate to the N3 nitrogen of A2451 in the ribosome relative to the corresponding proton-transfer reaction in aqueous solution.

In absence of a putitative general base for the ester aminolysis reaction, it was suggested that the peptidyl transferase center "accelerates the rate of the reaction it catalyzes by using the favourable energy of substrate binding to overcome the entropic cost of aligning substrates" (*23*), that the major contribution to catalysis "derives from simply positioning two reactive substrates in close proximity" (*11*), and even that "substrate orientation is the sole driving force behind the ribosome-catalyzed reaction" (*24*). The latter proposal was based on the thermodynamic analysis by Sievers et al. (*9*) who themselves, however, explicitly mentioned the possibility that the observed entropic advantage in the ribosome reaction compared to solution could also arise from reorganization effects of the surroundings (*9*).

Computer simulations of the peptidyl transfer reaction, yielding a value of $k_{cat} \simeq 2\ s^{-1}$, showed that it is precisely the reduced reorganization free energy in the ribosome, achieved through an intricate hydrogen bonding network, that is responsible for the more positive entropy of activation (*10*). The peptidyl transfer center could thus be viewed as a rather stiff H-bond network with preorganized dipoles that do not need major rearrangements during the reaction. Many of these hydrogen bonds, in particular those involving waters,

were not present in the single-substrate structures but were established spontaneously during MD simulations, thus, representing powerful predictions. The substrate alignment contribution, relative to the uncatalyzed reaction, was estimated to be less than about 1 kcal/mol in addition to the 2.4 kcal/mol associated with bringing the reactants to the same 55 M cage (for direct comparison with the solution reaction) (*10*). We note that our estimate of this (~3.4 kcal/mol) contribution is in good agreement with the independent results of Sharma et al. (*25*). Hence, the common belief that activation entropy can be directly equated to substrate translational and rotational motions is clearly not correct. The activation entropy measures the entropy change of the entire system, which, in addition to the reacting substrates, also includes the surrounding environment consisting of ribosomal groups, water molecules, ions, and so forth. It is therefore not warranted to interpret net entropy changes solely in terms of proximity and alignment concepts. Furthermore, as pointed out in ref *10*, the reduction in $-T\Delta S^{\ddagger}$ compared to the uncatalyzed reaction was also seen for the second-order k_{cat}/K_M rate constant that corresponds to the situation with *unbound* A-site puromycin substrate. This experimental result is therefore difficult to reconcile with the alignment proposal.

One of the main findings from the computer simulations was that the adenine 2′-OH group of the P-site substrate is able to support catalysis by direct participation in the reaction as a proton shuttle between the attacking amino group and leaving (3′) ester oxygen. This results in a six-membered transition state, as also found in refs *25*, *26*, where the 2′-OH donates its proton to the adjacent 3′ oxygen while simultaneously receiving one of the amino protons. As mentioned earlier, this mechanism explains experimental data regarding the inability of 2′-deoxy and 2′-substituted substrates to promote peptidyl transfer (*13*, *14*). It should, however, be noted that the involvement of the 2′-OH group does not constitute a catalytic effect per se, since such a group would presumably not render the corresponding solution reaction much faster, as its position can be taken equally well by a water molecule (*25*). Rather, our results showed that it is a precisely tuned hydrogen bond network supporting the transition state structure that is the main reason for catalysis (*10*). With this preorganized network, the ribosome can avoid the extensive solvent reorganization along the reaction, that is inevitable in the corresponding solution process, and this leads to a significantly more positive entropy of activation than what is seen for the uncatalyzed reaction.

Structural Predictions. The hydrogen bonding network predicted in ref *10* involves both ribosomal bases and several water molecules that can bridge the interactions between the substrates and polar groups of the ribosome. In particular, it was found that the apparent lack of any stabilizing interactions for the developing "oxyanion" of the transient tetrahedral intermediate in the X-ray structural models was explained by the penetration of water molecules into the active site. One critical water molecule was predicted to be situated between the bases of A2602, U2585, and the 2′-OH of U2584 (Figure 3a of ref *10*), and this water makes a strong hydrogen bond to the negative oxygen of the TI, thereby providing the missing stabilization of the TI. The newly determined crystal structures by Steitz and co-workers of the large *Haloarcula marismortui* ribosomal subunit in complex with transition state analogues (*6*, *7*) now confirm this prediction, and a water molecule is indeed found in the same position as in the MD simulations in both the 1VQP and 1VQ7 structures (Figure 2A).

Several other essential water molecules that bridge the interactions between the substrates and universally conserved ribosomal groups were also predicted from the MD simulations. One of them makes a hydrogen bond directly to the 2′-OH of the A-site A76, as well as to the C═O and 2′-OH groups of C2063 and to the N3 nitrogen of A2451 (Figure 3 of ref *10*). This water is now observed in both structures with TS analogues (*6*, *7*) (1VQP and 1VQ7), with the very same hydrogen bonding pattern as in the simulations (Figure 2B). Another water interacting with the one just mentioned and which makes hydrogen bonds to A76 N3 and C2063 O2′ is part of the H-bond network (Figure 3b of ref *10*) and is again now found in both the 1VQP and 1VQ7 crystal structures in exactly the predicted position (Figure 2B). Two additional water molecules in this region, extending out from the P-site, were also seen in the MD simulations (one is shown in Figure 3 of ref *10*), and these are situated approximately at the position where electron density interpreted as a K^+ ion is found in 1VQP and 1VQ7. Finally, a water molecule on the A-site side making H-bonds to the 2′-OH of A2451, the N6 nitrogen of A2602, and the carbonyl group of the attacking amino acid was predicted (Figure 3a of ref *10*), and this water is now seen in the same position in the 1VQ7 structure (*6*) (Figure 2C).

Another critical interaction predicted by the MD simulations is the hydrogen bond between the O2′ of A2451 and 2′-OH group of the P-site substrate (*10*). Obviously, all direct H-bonds to the 2′-OH proton shuttle are likely to be of considerable importance for the intramolecular proton-transfer mechanism. This particular interaction may therefore constitute one of the major effects of A2451 on the reaction, and it is possible that the conservation of A2451 reflects structural requirements for keeping its O2′ in the correct position, rather than implying a direct role of its base in the catalytic reaction (*10*, *27*, *40*). Our calculations showed that replacing A2451 with dA2451 yielded a destabilization of the transient intermediate by about 3 kcal/mol (*10*). The predicted H-bond between A2451 O2′ and the P-site substrate is also observed in the 1VQP structure (Figure 2C), although it is not discussed in ref *7*. In the 1VQ7 structure, on the other hand, this H-bond is naturally missing, since the last P-site nucleotide has a deoxyribose moiety (*6*).

Simulations Using New Crystal Structures. Already the fact that a number of critical interactions involving substrates, ribosomal groups, and water molecules could be correctly predicted essentially a priori, using modeling and combination of available structures and subsequent MD simulations, indicates that this procedure is indeed sufficiently reliable. It is, however, interesting to examine whether utilization of the new structures has any significant effects on the calculated results. We thus carried out MD/FEP/EVB simulations in the same manner as in ref *10* but now using the 1VQP structure as the initial model (see Materials and Methods). These calculations immediately show that the energetics is not particularly sensitive to the choice of initial structure. The free energy barriers corresponding to the two transition states appearing along the reaction are calculated

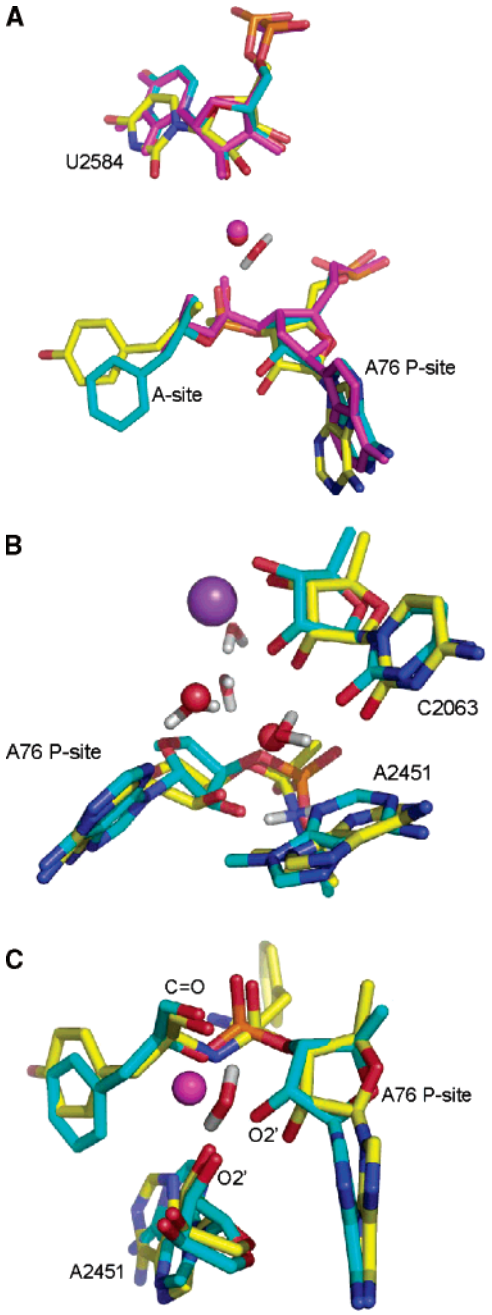

FIGURE 2: Predicted and observed water molecules in the peptidyl transfer center. (A) Comparison of the predicted position for the water molecule stabilizing the negative oxygen of the tetrahedral intermediate from MD simulations (*10*) (yellow) with the experimental positions in the 1VQP (cyan) and 1VQ7 (purple) structures (*6*, *7*). The MD water is shown in red and white, while the crystallographic ones are shown as solid spheres. (B) Comparison of the predicted positions of waters participating in the H-bond network (*10*) with experimental results (*7*) (MD, yellow; 1VQP, cyan). Crystallographic water molecules are depicted as red spheres, while the purple sphere is interpreted as a K^+ ion (*7*). (C) Comparison of the predicted (*10*) and observed positions (*6*) for a water molecule interacting with the 2′-OH of A2451 and the carbonyl group of the A-site substrate (MD, yellow; 1VQP, cyan). The crystallographic water position (solid sphere) is the from 1VQ7 structure (*6*).

to be 11.3 ± 0.6 kcal/mol and 17.3 ± 0.8 kcal/mol, respectively, compared to the earlier results of 10 and 17 kcal/mol (with estimated error bars of ±1.5 kcal/mol based on several independent simulations). Furthermore, the free energy of the transient tetrahedral intermediate is now

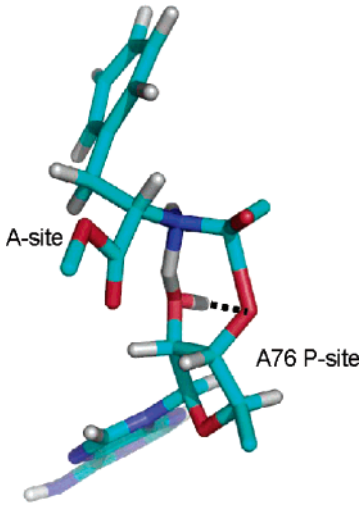

FIGURE 3: Snapshot from MD simulations in the transition state region from simulations starting from the 1VQP structure. The transition state structure is very insensitive to the choice of initial ribosome model.

predicted to be 9.1 ± 0.6 kcal/mol relative to the reactants, compared to 8 ± 1.5 kcal/mol obtained previously. The energetic results are thus very similar, and this is also reflected by the similarity of the highest transition state obtained, which corresponds to a mixture with about 60% of the TI and 40% of product resonance forms (Figure 3).

Both the present and earlier MD trajectories also suggest that C−O bond cleavage lags slightly behind deprotonation of the attacking nitrogen in the TS, so that proton transfer to the P-site O2′ is well-advanced in the transition structure. In this context, the recent work of Strobel and co-workers (*13*) should also be mentioned. They measured a normal primary ^{15}N kinetic isotope effect (1.0090−1.0097) for peptidyl transfer to a puromycin derivative in a slow 50S assay and proposed that formation on the C−N bond is actually rate-limiting (*13*). However, as is well-known, the interpretation of a mechanism from a single primary heavy atom isotope effect can be very uncertain, in particular with a nucleophile like nitrogen where protonation/deprotonation and hydrogen bonding effects tend to obscure the results (see, e.g., discussion in ref *28*). Hence, it seems impossible to determine a TS structure from such data in the absence of additional ester ^{18}O and possibly also H/D istope effects. Most data on ester aminolysis, as well as the reverse amide hydrolysis reactions, indicate that C−O bond breakage or protonation steps are usually rate-limiting (*25*, *28*−*31*), in agreement with our results. However, since the MD/EVB simulations show a late TS for C−N bond formation, as well as strong H-bonding between the nucleophile and the P-site O2′ before the proton is transferred, the geometry and charge distribution of the rate-limiting TS will be similar to that of the high energy intermediate, irrespective of whether it actually is located before or after the intermediate.

Role of Induced Fit. The new MD simulations starting from the 1VQP structure now also utilize experimental initial positions for the additional water molecules. Unsurprisingly, the H-bond network, as well as the locations of the relevant waters, remains intact throughout these simulations (data not shown) and agrees very well with our earlier predictions. The main difference between our earlier initial model and the new experimental TS analogue structures, however, is

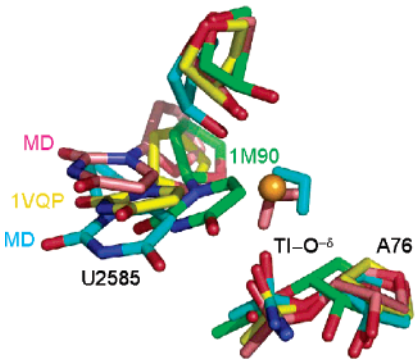

FIGURE 4: Comparisons of the motions of U2585 in MD simulations (cyan and pink) with the observed conformations of this base in the 1VQP (yellow) and 1M90 (green) structures.

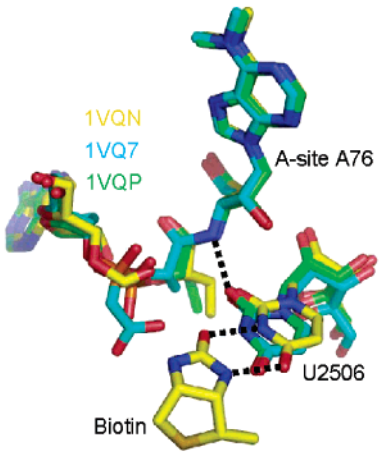

FIGURE 5: Hydrogen bonding between the puromycin NH group and U2506 in the three induced structures 1VQN (yellow), 1VQ7 (cyan), and 1VQP (green). H-bonding between the biotin headgroup and U2506 in 1VQN is also shown, and the apparent interaction between the TSA carboxylate group and U2506 in 1VQ7 can also be appreciated.

the orientation of the uracil residue U2506. In the recent work by Steitz' group (*6*), a conformational change of U2506 and also a smaller shift of U2585 were interpreted in terms of an "induced fit" mechanism for promoting peptidyl transfer and preventing hydrolysis of the P-site substrate. That is, these results suggested that upon going from a truncated A-site substrate without C74 to one containing the full CCA trinucleotide (or CC-hydroxypuromycin) an "induced state" of the active site was triggered. In the case of an aminoacylated A-site tRNA or CCA fragment, this induced fit would promote peptidyl transfer, while in the case of a deacylated A-site substrate, it would promote hydrolysis of the P-site ester bond. While this type of induced fit mechanism looks plausible, an obvious objection to it would be that puromycin itself, without C74 and C75, readily attacks the A-site substrate at a high rate (*8*) (the same goes for C-puromycin) (*32*). Thus, an induced fit mechanism where the conformational changes do not seem to be necessary for reaction makes the concept somewhat vague. It should also be noted that induced fit proposals, in general, do not explain the origin of catalytic effects but merely state that binding leads to an optimal arrangement for catalysis.

The essence of the above hypothesis both for peptidyl transfer and ester hydrolysis is that the position of U2585 in the uninduced state is such that it would protect the P-site ester carbon from attack by a nucleophile. However, the shift of this base between the uninduced and induced positions is rather small and in all our MD simulations the U2585 base is found to be fairly mobile and essentially spanning a range of conformations between the two states observed experimentally (Figure 4). In line with the result that puromycin reacts equally well with and without C74 (and C75) attached to it (*8*, *32*), we find virtually identical reaction energetics with the uninduced and induced positions of U2585 and U2506 as our starting conformations. The reason that the larger conformational change of U2506 would promote reaction with the amino group or hydrolysis by a water molecule is not entirely clear, and again, our results indicate that its effect is minor as far as peptidyl transfer is concerned. It is, of course, still possible that these conformational changes could play a more important role in hydrolysis of the P-site ester bond.

The use of transition state analogues for cocrystallization is obviously a very powerful tool for experimental analysis of mechanistic possibilities. In the present case, the new structures have given a first glimpse of what reaction intermediates would look like on the ribosome, and we find it extremely encouraging that the TS analogues superimpose so well on our predicted MD stuctures (Figures 2 and 4). One should, however, be aware of the possibility that substitution or addition of polar groups (change of polarity) in TS or substrate analogues may cause structural distortions, since it is not only the shape that makes an analogue. It is therefore interesting to note some pertinent features of the induced structures (*6*, *7*) 1VQN, 1VQ7, and 1VQP. In 1VQN, the capping biotin headgroup of the P-site substrate analogue makes two H-bonds to U2506 (N3 and C4═O) seemingly locking it into the induced conformation. In 1VQ7, in contrast, the "artificial" carboxylate group of the TS analogue apparently interacts with the U2506 NH group. In 1VQP, there is no direct hydrogen bonding between the uracil and the TS analgoue, but again, the NH group of U2506 is pointing between the two oxygens bearing the additional active site negative charge. Interestingly, in all these three structures, the O2 carbonyl of U2506 makes a strong H-bond to the NH group of the puromycin derivatives (Figure 5). Note that this NH group replaces the normal A-site A76 O3 ester oxygen. So, it seems possible that the "induced state" is not caused by the addition of the A-site C74 in these structures but by a combination of artificial groups of the analogues together with the puromycin 3′-NH group. In particular, the difference between the undinduced (1VQ6: CCApcb + ChPmn) and induced (1VQN: CCApcb + CChPmn) reactant analogue structures, where the latter contains C74, seems to be equally well-explained by the biotin interaction.

The recent results of Green and co-workers (*32*) show that reaction with the C75-puromycin substrate is not very sensitive to mutation of either U2506 or U2585, although it lacks C74. This finding seems difficult to reconcile with the proposed important role of C74 in inducing a reactive conformation for peptidyl transfer. In contrast, the most sensitive mutant with the fMetPheCpm substrate is U2506G, which seems to be the only substitution of U2506 that cannot place an H-bond acceptor for interaction with the puromycin NH group, and this interpretation would speak in favor of the "induced" conformation of U2506 as the reactive one

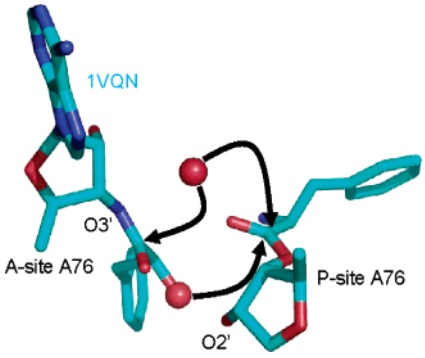

FIGURE 6: Hypothetical mechanisms for hydrolysis where attack on either the P-site or A-site aminoacyl ester bonds is considered based on the 1VQN crystal structure (*6*). The hydroxyl group of the CChPmn A-site substrate is depicted as a solid sphere to indicate the possible location of a hydrolytic water molecule when a deacylated A-site substrate is bound. The water molecule that is within range for attack on either ester carbon is also shown, although no acid−base pathway assisting it seems possible (see text).

with puromycin. The mutants of A2451, U2506, U2585, and A2602 studied by Green and co-workers also had very little effect with aminoacyl-tRNA as the A-site substrate, while they had large effects with puromycin substrates lacking C75 (*11*). This was interpreted such that these four universally conserved bases have no apparent role in peptide bond formation (*11*). It seems to us that this hypothesis is unnecessarily strong, considering that the assay used was not rate-limited by peptidyl transfer but by tRNA accommodation. That is, it seems that the effects of the mutations with real substrates could still be significant but smaller than for puromycin and, therefore, still not render peptidyl transfer rate-limiting.

Peptidyl-tRNA Hydrolysis. It seems established, however, that the A-site C74 has an effect on hydrolysis of the P-site substrate and that both full-length deacylated tRNAs (*33*, *34*) and the trinucleotide CCA (*33*) can promote hydrolysis of the P-site substrate. Exactly how the hydrolysis reaction (in the absence of release factors) would proceed is, however, not entirely obvious. The simplest interpretation of the reaction experiments would be that the 3′-OH of the (deacylated) A-site A76 is essential for positioning of a hydrolytic water molecule that would react by the same type of proton shuttle mechanism as for the amino group attack (Figure 6). Such a hydrolytic water could then be expected to be located approximately at the position of the hydroxyl group of the CChPmn A-site substrate in the 1VQN crystal structure (*6*) (Figure 6). Further, while CCA and longer sequences up to a full-length tRNA evidently bind to the A-site, it could be the case that the CA dinucleotide simply does not. In this type of scenario, the main issue is then what the minimal sequence is for binding to the A-site, and not necessarily possible conformational changes that may accompany binding. An alternative could, in principle, be that the water molecule stabilizing the negative oxygen in the peptidyl transfer TS (Figures 2A and 4) carries out hydrolysis of the P-site ester, but from the opposite face. This water is also within interaction distance to the 3′OH of a deacylated A-site ligand, but the main problem with such a mechanism is that there is no general acid−base for proton transfer to the leaving group. A curious fact that can also be observed is that this water molecule, both in the MD simulations and crystal structures (1VQN, 1VQ7, and 1VQP), looks to be in a very good position for attack on the A-site ester bond after peptidyl transfer (Figure 6). However, again, there seems to be no reasonable acid−base pathway leading to deprotonation of the nucleophile and protonation of the leaving group. Also, ester hydrolysis is considerably slower than the reverse aminolysis reaction with a free energy barrier that is approximately 8 kcal/mol higher in solution. Hence, spontaneous hydrolysis is, fortunately, bound to be slow, and it is therefore logical that additional elements (release factors) are required to speed it up.

CONCLUDING REMARKS

Taken together, the number of predictions from MD simulations of the ribosomal peptidyl transfer reaction that are supported and verified by experimental data is impressive. These include predictions of the now confirmed hydrogen bonding network, essential water positions, and the stereochemistry of the tetrahedral intermediate (*S*-enantiomer), as well as the overall energetics of the reaction and the interesting activation entropy effect discussed in the Introduction. The results show that critical structural features can be obtained from the simulations using initial models where these features were not present. This does not mean that MD sampling generally can predict details of macromolecular structures from scratch, but given a reasonable initial model, the technique can evidently be very useful for sampling and refining structures from such a model. Importantly, the computational methodology also provides a direct route for converting 3D structural information to quantitative energetics, which is often missing. Computer simulations are indeed playing an increasingly important role in advancing our understanding of biological catalysis (*35*−*37*), and our results show that reaction calculations of the present type can provide important links between structure and function, even for complex systems such as the ribosome. This opens up the possibility of elucidating energetic relationships that are very difficult to address experimentally.

While the general mechanism for ribosomal peptidyl transfer now seems to be essentially established, through combined efforts of experiments and computations, a number of interesting observations remain unexplained. These include the different sensitivities of the puromycin versus the C75-puromycin and aminoacyl-tRNA reactions to mutations at the four positions A2451, U2506, U2585, and A2602 (*11*, *32*). Whether these effects are really indicating different interactions depending on A-site substrates or whether they are masked by a change of rate-limiting step is important to clarify. It should also be of interest to understand the possible effect on kinetics of substituting the native tRNA ester bond with the puromycin amide linkage, which affects both polarity and rigidity at the A-site attachment point. Another issue that at present seems puzzling is the reported rate differences between P-site substrates of different length and/or with different amino acids attached to the tRNA (*8*, *32*). As far as the effect of the length of the P-site peptide is concerned, we find no significant difference between our present and earlier calculations with a dipeptide and a tripeptide, respectively. This appears to be consistent with the results of Katunin et al. (*8*) who only find a factor of 2 difference in the peptidyl transfer rates with fMetPhe-tRNA and fMetPhePhe-tRNA P-site substrates, which is within the

errors of our calculated activation free energies. In contrast, the observed rate difference between fMet-tRNA and fMetAlaAsnMetPheAla-tRNA is about a factor of 50−100 which is a rather large effect (*8*), the origin of which is not clear but certainly interesting. Finally, the origin of the 1.5 slope dependence of the peptidyl transfer rate (log k_{pep}) on pH with a second pK_{a2} of 7.5−8 (*8*, *22*), that has now been shown to not be affected by mutation of A2451 (*22*), remains elusive, although some type of pH-dependent conformational change could provide an explanation.

With the peptidyl transfer mechanism reasonbly well-understood, the details of the peptidyl-tRNA hydrolysis process on the ribosome, both with and without the help by release factors (RFs), presents one of the major mechanistic problems to resolve. To apply our computer simulation scheme to the hydrolysis reaction without release factors is relatively straightforward, but also in the RF-assisted case does it seem worthwhile to try to apply a computational approach to the problem in conjunction with new structural data. X-ray and cryo-EM structures of ribosomal complexes with release factors have recently emerged, and although the resolution still does not give atomic detail of the RF-codon and RF-peptidyl transfer center interactions, the approximate locations of the important P(A/V)T (in RF1), SPF (in RF2), and GGQ motifs can now be seen (*38*, *39*). It seems possible, for example, that standard peptide docking procedures could be employed to explore possible conformations of the relevant protein loops using the experimental structural data as constraints. This could then be used to generate sets of putative structures for further evaluation by more detailed energetic calculations.

ACKNOWLEDGMENT

We thank Profs. Marina Rodnina and Måns Ehrenberg for useful discussions.

REFERENCES

1. Ban, N., Nissen, P., Hansen, J., Moore, P. B., and Steitz, T. A. (2000) The complete atomic structure of the large ribosomal subunit at 2.4 Å resolution, *Science 289*, 905−919.
2. Harms, J., Schluenzen, F., Zarivach, R., Bashan, A., Gat, S., Agmon, I., Bartels, H., Franceschi, F., and Yonath, A. (2001) High-resolution structure of the large ribosomal subunit from a mesophilic eubacterium, *Cell 107*, 679−688.
3. Hansen, J. L., Schmeing, T. M., Moore, P. B., and Steitz, T. A. (2002) Structural insights into peptide bond formation, *Proc. Natl. Acad. Sci. U.S.A.* 99, 11670−11675.
4. Schmeing, T. M., Seila, A. C., Hansen, J. L., Freeborn, B., Soukup, J. K., Scaringe, S. A., Stobel, S. A., Moore, P. B., and Steitz, T. A. (2002) A pre-translocational intermediate in protein synthesis observed in crystals of enzymatically active 50S subunits, *Nat. Struct. Biol. 9*, 225−230.
5. Nissen, P., Hansen, J., Ban, N., Moore, P. B., and Steitz, T. A. (2000) The structural basis of ribosome activity in peptide bond synthesis, *Science 289*, 920−930.
6. Schmeing, T. M., Huang, K. S., Strobel, S. A., and Steitz, T. A. (2005) An induced-fit mechanism to promote peptide bond formation and exclude hydrolysis of peptidyl-tRNA, *Nature 438*, 520−524.
7. Schmeing, T. M., Huang, K. S., Kitchen, D. E., Strobel, S. A., and Steitz, T. A. (2005) Structural insights into the roles of water and the 2′ hydroxyl of the P site tRNA in the peptidyl transferase reaction, *Mol. Cell 20*, 437−448.
8. Katunin, V. I., Muth, G. W., Strobel, S. A., Wintermeyer, W., and Rodnina, M. V. (2002) Important contribution to catalysis of peptide bond formation by a single ionizing group within the ribosome, *Mol. Cell 10*, 339−346.
9. Sievers, A., Beringer, M., Rodnina, M. V., and Wolfenden, R. (2004) The ribosome as an entropy trap, *Proc. Natl. Acad. Sci. U.S.A.* 101, 7897−7901 and 12397−12398.
10. Trobro, S., and Åqvist, J. (2005) Mechanism of peptide bond synthesis on the ribosome, *Proc. Natl. Acad. Sci. U.S.A.* 102, 12395−12400.
11. Youngman, E. M., Brunelle, J. L., Kochaniak, A. B., and Green, R. (2004) The active site of the ribosome is composed of two layers of conserved nucleotides with distinct roles in peptide bond formation and peptide release, *Cell 117*, 589−599.
12. Weinger, J. S., Parnell, K. M., Dorner, S., Green, R., and Strobel, S. A. (2004) Subsrate-assisted catalysis of peptide bond formation by the ribosome, *Nat. Struct. Biol. 11*, 1101−1106.
13. Seila, A. C., Okuda, K., Núnes, S., Seila, A. F., and Strobel, A. S. (2004) Kinetic isotope effect analysis of the ribosomal peptidyl transferase reaction, *Biochemistry 44*, 4018−4027.
14. Quiggle, K., Kumar, G., Ott, T. W., Ryu, E. K., and Chládek, S. (1981) Donor site of ribosomal peptidyltransferase: Investigation of substrate specificity using 2′(3′)-*O*-(*N*-acylaminoacyl)dinucleoside phosphates as models of the 3′ terminus of *N*-acylaminoacyl transfer ribonucleic acid, *Biochemistry 20*, 3480−3485.
15. Marelius, J., Kolmodin, K., Feierberg, I., and Åqvist, J. (1998) Q: A molecular dynamics program for free energy calculations and empirical valence bond simulations in biomolecular systems, *J. Mol. Graphics 16*, 213−225.
16. MacKerell, A. D., Jr., Wiórkiewicz-Kuczera, J., and Karplus, M. (1995) An all-atom empirical energy function for the simulation of nucleic acids, *J. Am. Chem. Soc. 117* 11946−11975.
17. King, G., and Warshel, A. (1989) A surface constrained all-atom solvent model for effective simulations of polar solutions, *J. Chem. Phys. 91*, 3647−3661.
18. Lee, F. S., and Warshel, A. (1992) A local reaction field method for fast evaluation of long-range electrostatic interactions in molecular simulations, *J. Chem. Phys. 97*, 3100−3107.
19. Warshel, A. (1991) *Computer Modeling of Chemical Reactions in Enzymes and Solutions*, Wiley-Interscience, New York.
20. Åqvist, J., and Warshel, A. (1993) Simulations of enzyme reactions using valence bond force fields and other hybrid quantum/classical approaches, *Chem. Rev. 93*, 2523−2544.
21. Muth, G. W., Ortoleva-Donnelly, L., and Strobel, S. A. (2000) A single adenosine with a neutral pK_a in the ribosomal peptidyl transferase center, *Science 289*, 947−950.
22. Beringer, M., Bruell, C., Xiong, L., Pfister, P., Bieling, P., Katunin, V. I., Mankin, A. S., Böttger, E. C., and Rodnina, M. V. (2005) Essential mechanisms in the catalysis of peptide bond formation on the ribosome, *J. Biol. Chem. 280*, 36065−36072.
23. Moore, P. B., and Steitz, T. A. (2003) After the ribosome structures: how does peptidyl transferase work? *RNA 9*, 155−159.
24. Gregory, S. T., and Dahlberg, A. E. (2004) Peptide bond formation is all about proximity, *Nat. Struct. Mol. Biol. 11*, 586−587.
25. Sharma, P. K., Xiang, Y., Kato, M., and Warshel, A. (2005) What are the roles of substrate-assisted catalysis and proximity effects in peptide bond formation by the ribosome? *Biochemistry 44*, 11307−11314.
26. Das, G. K., Bhattacharyya, D., and Burma, D. P. (1999) A possible mechanism of peptide bond formation on the ribosome without mediation of peptidyl transferase, *J. Theor. Biol. 200*, 193−205.
27. Erlacher, M. D., Lang, K., Shankaran, N., Wotzel, B., Huttenhofer, A., Micura, R., Mankin, A. S., and Polacek, N. (2005) Chemical engineering of the peptidyl transferase center reveals an important role of the 2′-hydroxyl group of A2451, *Nucleic Acid Res. 33*, 1618−1627.
28. Anderson, V. E., Cassano, A. G., and Harris, M. E. (2006) In *Isotope Effects in Chemistry and Biology* (Kohen, A., Limbach, H.-H., Eds.), pp 893−914, CRC Press, Boca Raton, Fl..
29. Strajbl, M., Florián, J., and Warshel, A. (2000) Ab initio evaluation of the potential surface for general base-catalyzed methanolysis of formamide: a reference solution reaction for studies of serine proteaser, *J. Am. Chem. Soc. 122*, 5354−5366.
30. Kaminski, Z. J., Paneth, P., and O'Leary, M. H. (1991) Nitrogen kinetic isotope effects on the acylation of aniline, *J. Org. Chem. 56*, 5716−5718.

31. Sawyer, C. B., and Kirsch, J. F. (1973) Kinetic isotope effects for reactions of methyl formate-*methoxyl*-$^{18}O^{1}$, *J. Am. Chem. Soc. 95*, 7375−7381.
32. Brunelle, J. L., Youngnan, E. M., Sharma, D., and Green, R. (2006) The interaction between C75 of tRNA and the A loop of the ribosome simulates peptidyl transferase activity, *RNA 12*, 33−39.
33. Caskey, C. T., Beaudet, A. L., Scolnick, E. M., and Rosman, M. (1971) Hydrolysis of fMet-tRNA by peptidyl transferase, *Proc. Natl. Acad. Sci. U.S.A. 68*, 3163−3167.
34. Zavianov, A. V., Mora, L., Buckingham, R. H., and Ehrenberg, M. (2002) Release of peptide promoted by the GGQ motif of class 1 release factors regulates the GTPase activity of RF3, *Mol. Cell 10*, 789−798.
35. Warshel, A. (2003) Computer simulations of enzyme catalysis: methods, progress, and insights, *Annu. Rev. Biophys. Biomol. Struct. 32*, 425−443.
36. Garcia-Viloca, M., Gao, J., Karplus, M., and Truhlar, D. G. (2004) How enzymes work: analysis by modern rate theory and computer simulations, *Science 303*, 186−195.
37. Bjelic, S., and Åqvist, J. (2004) Computational prediction of structure, substrate, binding mode, mechanism and rate for a malaria protease with a novel type of active site, *Biochemistry 43* (46), 14521−14528.
38. Petry, S., Brodersen, D. E., Murphy, F. V., Dunham, C. M., Selmer, M., Tarry, M. J., Kelley, A. C., and Ramakrishnan, V. (2005) Crystal structures of the ribosome in complex with release factors RF1 and RF2 bound to a cognate stop codon, *Cell 123*, 1255−1266.
39. Rawat, U., Gao, H., Zavialov, A., Gursky, R, Ehrenberg, M., and Frank, J. (2006) Interactions of the release factor RF1 with the ribosome as revealed by cryo-EM, *J. Mol. Biol. 357*, 1144−1153.
40. Erlacher, M. D., Lang, K., Wotzel, B., Rieder, R., Micura, R., and Polacek, N. (2006) Efficient ribosomal peptidyl transfer critically relies on the presence of the ribose 2′-OH at A2451 of 23S rRNA, *J. Am. Chem. Soc. 128*, 4453−4459.

BI0605383